TerraSAR-X / TanDEM-X

Ground Segment

Bandwidth Considerations in Range and Azimuth for Interferometric Applications

Microwaves and Radar Institute

&

Remote Sensing Technology Institute

prepared:

Michele Martone, Carolina Gonzalez and Sergi Duque
Date
Performance Engineer, Performance Engineer and ITP Developer

reviewed:

B. Bräutigam Date
System Performance Engineer

approved:

T. Fritz Date
ITP Manager

released:

M. Zink Date
GS Project Manager

DOCUMENT PREPARATION

The document on hand was prepared with contributions from the personnel listed below:

Name (name, surname)	Organizational Unit
Microwaves and Radar Institute (DLR-HR)	
Gonzalez, Carolina	HR - Satellite SAR Systems
Martone, Michele	HR - Satellite SAR Systems
Bräutigam, Benjamin	HR - Satellite SAR Systems
Remote Sensing Technology Institute (DLR-IMF)	
Duque, Sergi	IMF – SAR Signal Processing
Fritz, Thomas	IMF – SAR Signal Processing

DISTRIBUTION

This document is intended for public access.
Custodian of this document is: S. Duque

DOCUMENT CHANGE CONTROL

This document is under configuration control. Latest changes to the document are listed first.

Issue	Date	Chapter	Changes
1.0	26.06.2015	All	First issue

Note: Verify that this is the correct revision before use. Check the document server for the latest version. Hardcopies of distributed documents are not updated automatically.

TABLE OF CONTENTS

1 Introduction

1.1 Purpose

Interferometric SAR (InSAR) exploits the phase difference of at least two complex-valued SAR images acquired from different orbit positions and/or at different times (single-pass with displaced center or multi-pass).

This document is intended to clarify when the range spectral filtering is carried out in the CoSSC (Coregistered Single look Slant range Complex) products generated during TanDEM-X Science Phase. The parameters in the annotation files that indicate the CoSSC has not been filtered are described in this document. In addition, a brief explanation is given in case the science user desires to perform a range filtering by its own.

The present document provides also an overview of the impact of the used bandwidth in range and in azimuth as well as of the interferometric resolution on ***the interferometric phase error*** for acquisitions with the TanDEM-X system. The values of bandwidth in range are to be used in the commanding of the transmitted chirp pulses. The azimuth bandwidth can be adapted by accordingly processing the complex-valued SAR images. The derived bandwidths should be taken as a recommendation.

1.2 Scope

This document is oriented to the scientific use of interferometric TanDEM-X data with focus on quad-polarization data and constraints from the bistatic science phase with large horizontal baselines. The scope of recommendations comprises the optimization with respect to interferometric data and not to individual SAR image e.g. the signal-to-noise ratio. This document complements the previous Technical Note (TN) ***"CoSSC Generation and Interferometric Considerations"*** [7].

This document is made available to the user community which has access to TanDEM-X Science Phase Products. Thus, it is addressed to SAR experts who are already familiar with InSAR processing.

The conclusions and graphics from Section 5 to 8 can be applied to all acquisitions performed during the bistatic science phase with large horizontal baselines. Section 9 focuses on the impact on Quad polarization acquisitions and on the optimization of the processing bandwidths for this specific acquisition mode.

2 References

2.1 Applicable references

The following documents are fully applicable together with this document.

	Document ID	Document Title	Issue

2.2 Normative references

The following standards have been used for preparing the plan on hand.

	Document ID	Document Title	Issue

2.3 Informative references

The following documents, though not formally part of this document, amplify or clarify its content.

	Document ID	Document Title	Issue
[1]	TD-PD-PL-0032	I. Hajnsek, T. E. Busche, "Announcement of Opportunity – TanDEM-X Science Phase", Public Technical Note, May 2014	3.0
[2]	TD-GS-PS-3028	TanDEM-X Experimental Product Description	1.2
[3]		F. Gatelli, A. M. Guarnieri, F. Parizzi, P. Pasquali, C. Prati, and F. Rocca, "The wavenumber shift in SAR interferometry," IEEE Trans. Geosci. Remote Sens., vol. 32, no. 4, pp. 855–865, July 1994.	
[4]		G. Krieger, A. Moreira, H. Fiedler, I. Hajnsek, M. Werner, M. Younis, and M. Zink, "TanDEM-X: A satellite formation for high-resolution SAR interferometry," IEEE Trans. Geosci. Remote Sens., vol. 45, no. 11, pp. 3317–3341, November 2007.	
[5]		J.-S. Lee, K. W. Hoppel, S. A. Mango, and A. R. Millerand, "Intensity and phase statistics of multilook polarimetric and interferometric SAR imagery," IEEE Trans. Geosci. Remote Sens., vol. 32, no. 5, pp. 1017–1028, September 1994.	
[6]		M. Martone, B. Bräutigam, P. Rizzoli, C. Gonzalez, M. Bachmann, and G. Krieger, "Coherence evaluation of TanDEM-X interferometric data," ISPRS J. of Photogr. Remote Sens., vol. 73, pp. 21–29, September 2012.	
[7]	TD-PGS-TN-2129	S. Duque, U. Balss, C. Rossi, T. Fritz and W. Balzer, "CoSSC Generation and Interferometric Considerations" ", Public Technical Note, July 2012	1.0
[8]		M. Gabele, B. Bräutigam, D. Schulze, U. Steinbrecher, N. Tous-Ramon, M. Younis, „Fore and Aft Channel Reconstruction in the TerraSAR-X Dual Receive Antenna Mode", IEEE Transactions on Geoscience and Remote Sensing, vol. 48 , Issue 2, pp. 795-806, 2010.	
[9]		S. Suchandt, H. Runge, H. Breit, U. Steinbrecher, A. Kotenkov, U. Balss, "Automatic Extraction of Traffic Flows Using TerraSAR-X Along-Track Interferometry", IEEE Transaction on Geoscience and Remote Sensing, vol.	

		48, no. 2, pp. 807-819, 2010	

3 Terms, definitions and abbreviations

Note: Terms, definitions and abbreviations with relevance to the overall project are to be entered into the central project glossary maintained on the "GS Information Server" under "Terms".

Terms, definitions and abbreviations with no relevance to the overall project, but necessary to understand the document on hand, may be listed below.

3.1 Terms and Definitions

Term	Definition

3.2 Abbreviations

Abbreviation	Meaning
AASR	Azimuth Ambiguity-to-Signal Ratio
ATI	Along-Track interferometry
BW	Bandwidth
DEM	Digital Elevation Model
DRA	Dual-Receive Antenna
FAASR	First Azimuth Ambiguity-to-Signal Ratio
MTI	Moving Target Indication
PBW	Processed Azimuth Bandwidth
PSI	Persistent Scatterer Interferometry
SNR	Signal-to-Noise Ratio
SRA	Single-Receive Antenna

4 TanDEM–X Science Phase schedule

The TanDEM–X Science Phase is described in [1]. The following table is an extract of the cited document, and represents the Science Phase Timeline regarding the operational mode and the across-track baselines.

Months 2104/15	**1 Oct**	**2 Nov**	**3 Dec**	**4 Jan**	**5 Feb**	**6 Mar**	**7 Apr**	**8 May**	**9 Jun**	**10 Jul**	**11 Aug**	**12 Sep**	**13 Oct**	**14 Nov**	**15 Dec**
Operation Mode	**Pursuit Monostatic**					**Bistatic**									
Baseline (values for all latitudes)	0-750 m (perp. baseline) (slow drift over 5 months)					3-4 km at Equa tor	3-4 km (horizontal baseline at Equator) smaller at higher latitudes (stable baselines over the whole period)					Fast drift back to 300 m	0-250 m (stable short perp. baselines)		
Spectral Range Filtering	Activated					No acquisitions	Deactivated					No acquisitions	Activated		

Table 1. Science Phase Timeline. Operational mode & across – track baselines.

During the 15 months duration of the Science Phase, two main operational modes are employed: Pursuit Monostatic and Bistatic. The Pursuit Monostatic phase covers the 5 firsts months, from October 2014 to February 2015. During this phase the CoSSC product generation is as usual and the spectral range filtering is activated [2][7]. The Bistatic phase goes from March to December 2015. This phase is divided into two sub-phases: the “large baseline” and the “short baseline” one. For the short baseline sub-phase baselines between 0 and 250 m are typically used. During this sub-phase, the spectral range filtering is activated, as done in the previous Pursuit Monostatic phase. On the other hand, the large baseline sub-phase is characterized by a fixed orbit formation with large baselines. The maximum is reached at the Equator with a geometrical normal baselines of 3 to 4 km. Notice that in the bistatic mode the effective normal baselines are half of geometrical, i.e. 1.5 to 2 km at the Equator. In the large baselines sub-phase the range spectral shift filter is deactivated due to a significant non-common bandwidth between the two interferometric channels. Consequently, the CoSSC products is delivered with full range bandwidth without any range spectral shift filtering.

5 Spectral shift impact in the bistatic large baseline phase

According to [3] the range spectral shift between two acquisitions due to their geometry is given by

$$\Delta f = -\frac{c_0 \cdot B_{n,eff}}{2 \cdot R_0 \cdot \tan(\theta - \alpha)}, \tag{1}$$

where c_0 is the light velocity, $B_{n,eff}$ is the effective baseline, R_0 is the range, λ is the wavelength, θ is the incidence angle, and α represents the local slope. Figure 5.1 shows the spectral shift for flat terrain (Figure 5.1a) and a local terrain slope of 10 degrees facing the sensor (Figure 5.1b) as a function of the effective baseline and of the incidence angle.

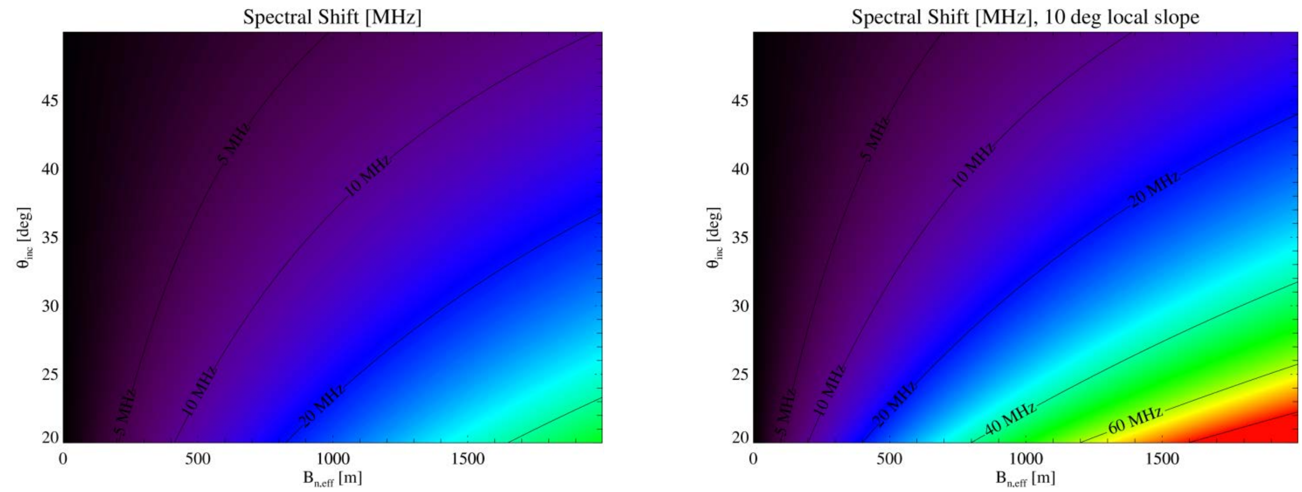

(a) (b)

Figure 5.1 Range spectral shift for flat terrain (a) and a local terrain slope of 10 degrees facing the sensor (b), considering the typical effective baseline values taking place in the bistatic phase and a range of incidence angles.

As it is illustrated in Figure 5.1, the spectral shift can be in the order of some tens of MHz for the large baselines occurring close to the equator. In addition, positive local slopes can significantly increase the range spectral shift, so that the spectral shift can become comparable with the total transmitted bandwidth and therefore approaching the total spectral separation. The range filtering in this case implies a significant loss of information which may be not desirable by some applications. Applications oriented to point targets, such as urban tomography or persistent scatterer interferometry (PSI), would prefer to keep the total original information without any information loss. Hence, the CoSSC products acquired during the bistatic large baseline phase preserve the signal information by ***not filtering in range***. If the user desires to have the channels filtered in range for his specific application, the filtering has to be carried out by himself. Section 6.2 explains briefly some considerations to be taken into account.

6 Practical considerations

6.1 Range filtering information in TanDEM-X CoSSC products annotation

A CoSSC which has not been filtered in range can be easily identified through the annotation on the provided XML description files. The main CoSSC XML description (TDM1_SAR__COS_HHHH_CC_D_EEE_xxxxxxxxTxxxxxx_yyyyyyyyTyyyyyy.xml [2]) file contains all the processing steps carried out during the InSAR processing. The range spectral filtering step can be found on the field <cossc_product><productInfo><processingStepsPerformed> <spectralFilteringRange>. The field value is set to "**true**" or "**false**" whether the range spectral filtering is activated or deactivated, respectively (see the example in Figure 6.1)

```
- <productInfo>
    <productType>COSSC</productType>
    <productVariant>standard</productVariant>
  - <processingStepsPerformed>
      <bistaticCorrections>true</bistaticCorrections>
      <coregistration>true</coregistration>
      <spectralFilteringAzimuth>true</spectralFilteringAzimuth>
      <spectralFilteringRange>false</spectralFilteringRange>
      <interferogramGeneration>true</interferogramGeneration>
      <phaseUnwrapping>true</phaseUnwrapping>
      <phaseUnwrappingDualBL>false</phaseUnwrappingDualBL>
      <phaseUnwrappingMultiBL>false</phaseUnwrappingMultiBL>
      <rawDEMGeneration>true</rawDEMGeneration>
    </processingStepsPerformed>
  </productInfo>
```

Figure 6.1 Main CoSSC XML description file in the case the Range Spectral Shift Filtering is deactivated.

The spectral filter XML descriptor is modified as well. This XML is located in the "***COMMON_ANNOTATION***" directory under the name "***spectral_filter_frequencies.xml***" (the XML description is provided in Annex A). In particular, the field <spectralShiftFilter_Block> <filteringConfig> <rangeFiltering> is accordingly set to "Activated"or "Deactivated"

6.2 How to perform spectral range filtering on TanDEM-X interferometric data

The user is free to perform the range spectral shift filtering by its own. The filter has to be applied locally since it is slope dependent. Therefore, the user has to estimate the local slopes in order to properly perform the filtering. For this, an external DEM or the coarse DEM provided within each SSC in the XML file "***georef.xml***" may be used. This file is located in the "***ANNOTATION***" directory inside each SSC. Notice that, since the bistatic passive channel has been coregistrated, the "***georef.xml***" to be used should be the one related to the monostatic active channel. The user should expect a worsening in the range resolution after the filtering process. Figure 6.2 illustrates the expected range resolution after applying the range spectral shift filter over a stripmap bistatic acquitision with 100 MHz range bandwidth. The corresponding slant range resolution before filtering is 1.76 m. Again, the calculation has been done for flat terrain (Figure 6.2a) and a local terrain slope (facing the radar sensor) of 10 degrees (Figure 6.2b) considering a wide range of incidence angles and large effective baselines.

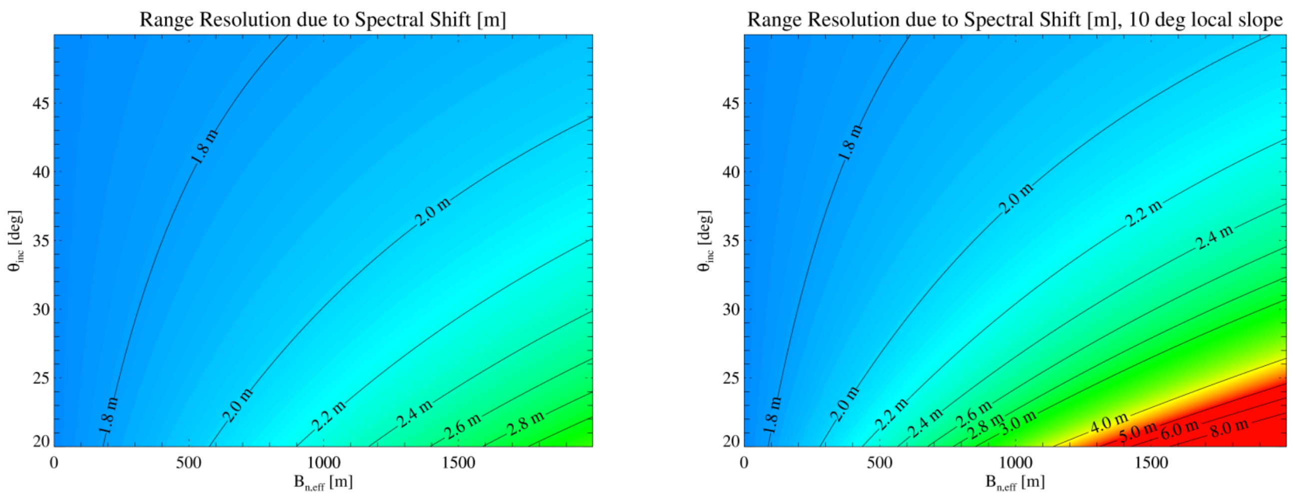

(a) *(b)*

Figure 6.2 Expected range resolution when filtering for a transmitted range bandwidth of 100 MHz in the case of (a) flat terrain and (b) 10 degree slope facing the radar sensor.

6.3 Dual Receive Antenna (DRA) - ATI acquisitions: azimuth filtering and annotation information

The bistatic data acquired in Dual Receive Antenna (DRA) - ATI mode preserves the azimuth processed bandwidth without any kind of spectral tapering for the DRA Aft and Fore images [8], [9]. In this case, neither antenna pattern compensation nor spectral windowing are applied. The purpose is to preserve full information for Moving Target Indication (MTI) and Along-Track Interferometry (ATI) applications in DRA configuration. Therefore, both interferometric combinations of Aft and Fore channels are not azimuth filtered.

Additionally to the Aft and Fore data, Single Receive Antenna (SRA) image pairs can be generated from a DRA acquisition in ATI mode. These SRA images are processed with their corresponding antenna pattern compensation and hamming azimuth windows. Thus, also their interferometric combination in the CoSSC product is azimuth filtered.

Notice that the main CoSSC XML description file is referred to the interferometric combination of the corresponding active and passive SRA channel. Therefore, in the main XML CoSSC file the spectral azimuth filtering is activated and the hamming coefficients for the interferogram generation are provided. Figure 6.3 shows an example of the main XML CoSSC descriptor file where the "***spectralFilteringAzimuth***" field is set to "***true***" value and the "***spectralFiltering***" contains the fields related to the parameters for the employed range and azimuth windowing.

```
-<cossc_product>
  +<generalHeader fileName="TDM1_SAR__COS_BIST_SM_S_DRA_20140310T171812_20140310T171818.
  +<productComponents></productComponents>
  -<productInfo>
     <productType>COSSC</productType>
     <productVariant>standard</productVariant>
    -<processingStepsPerformed>
       <bistaticCorrections>true</bistaticCorrections>
       <coregistration>true</coregistration>
       <spectralFilteringAzimuth>true</spectralFilteringAzimuth>
       <spectralFilteringRange>false</spectralFilteringRange>
       <interferogramGeneration>true</interferogramGeneration>
       <phaseUnwrapping>true</phaseUnwrapping>
       <phaseUnwrappingDualBL>false</phaseUnwrappingDualBL>
       <phaseUnwrappingMultiBL>false</phaseUnwrappingMultiBL>
       <rawDEMGeneration>true</rawDEMGeneration>
     </processingStepsPerformed>
   </productInfo>
  +<commonAcquisitionInfo></commonAcquisitionInfo>
  +<commonSceneInfo></commonSceneInfo>
  +<baselineInfo></baselineInfo>
  -<processingInfo>
    +<inputData></inputData>
    +<bistaticProcessing></bistaticProcessing>
    +<coregistration></coregistration>
    -<spectralFiltering>
       <azimuthBandwidthInCenter>2.75360926225091316E+03</azimuthBandwidthInCenter>
       <rangeBandwidthInCenter>1.00000000000000000E+08</rangeBandwidthInCenter>
       <azimuthHammingCoef>5.99999999999999978E-01</azimuthHammingCoef>
       <rangeHammingCoef>5.99999999999999978E-01</rangeHammingCoef>
     </spectralFiltering>
    +<inSARProcessing></inSARProcessing>
   </processingInfo>
  +<productQuality></productQuality>
 </cossc_product>
```


Figure 6.3 Example of main XML descriptor file referred to the CoSSC derived from a DRA acquisition.

image_layers	INT_32	3
image_layer_index	INT_32	1
image_layer_pol_sat1	STR	"HH"
image_layer_pol_sat2	STR	"HH"
image_layer_dra_sat1	STR	"SRA"
image_layer_dra_sat2	STR	"SRA"
image_layer_beam_sat1	STR	"strip_012"
image_layer_beam_sat2	STR	"strip_012"
insar_layer_index	INT_32	1

(a)


```
-<spectralShiftFilter_Block>
  -<blockConfig>
     <rangeSize>16366</rangeSize>
     <rangeOverlap>0</rangeOverlap>
     <azimuthSize>4096</azimuthSize>
     <azimuthOverlap>511</azimuthOverlap>
   </blockConfig>
  -<filteringConfig>
     <rangeFiltering>Deactivated</rangeFiltering>
     <azimuthFiltering>Activated</azimuthFiltering>
   </filteringConfig>
  +<scene name="FILT.1"></scene>
  +<scene name="FILT.2"></scene>
 </spectralShiftFilter_Block>
```


(b)

Figure 6.4 "image_layer_info.txt" (a) and "spectral_filter_frequencies.xml"(b) for a SRA – SRA interferometric pair.

The "***image_layer_info.txt***" ASCII file located also on the "***COMMON_ANNOTATION***" directory gives basic information related to the polarization, beam and antenna mode of the specific image layer in the current subdirectory. Figure 6.4a represents an example of the "***image_layer_info.txt***" for a SRA – SRA while Figure 6.4b shows its correspondent "***spectral_filter_frequencies.xml***" file. As mentioned before, in that case the spectral azimuth filtered is ***"Activated"***.
On the other hand, the interferometric combinations with Aft or Fore images are neither filtered norwindowed. Consistently, the field "***azimuthFiltering***" in the correspondent "***spectral_filter_frequencies.xml***" is set to "***Deactivated***". Figure 6.5 illustrates the "***image_layer_info.txt***" (a) for a Fore-Fore combination and its "***spectral_filter_frequencies.xml***" (b).

```
image_layers            INT_32   3
image_layer_index       INT_32   2
image_layer_pol_sat1    STR      "HH"
image_layer_pol_sat2    STR      "HH"
image_layer_dra_sat1    STR      "DRAFore"
image_layer_dra_sat2    STR      "DRAFore"
image_layer_beam_sat1   STR      "strip_012"
image_layer_beam_sat2   STR      "strip_012"
insar_layer_index       INT_32   2
```

(a)


```
-<spectralShiftFilter_Block>
 -<blockConfig>
    <rangeSize>16366</rangeSize>
    <rangeOverlap>0</rangeOverlap>
    <azimuthSize>4096</azimuthSize>
    <azimuthOverlap>511</azimuthOverlap>
  </blockConfig>
 -<filteringConfig>
    <rangeFiltering>Deactivated</rangeFiltering>
    <azimuthFiltering>Deactivated</azimuthFiltering>
  </filteringConfig>
 +<scene name="FILT.1"></scene>
 +<scene name="FILT.2"></scene>
 </spectralShiftFilter_Block>
```


(b)

Figure 6.5“image_layer_info.txt” (a) and “spectral_filter_frequencies.xml” (b) for a Fore-Fore interferometric pair.

7 Interferometric phase error

The key parameter for evaluating the interferometric performance is the phase error between the two interferometric SAR channels $\Delta\varphi$. The phase error depends on the coherence γ and the number of independent looks n. Its probability density function (pdf) can be expressed as a nonlinear function of both parameters [4], [5] :

$$P_{sp}(\varphi,\gamma,n) = \frac{\Gamma(n+1/2)(1-\gamma^2)\gamma\cos(\varphi)}{2\sqrt{\pi}\,\Gamma(n)(1-\gamma^2\cos^2(\varphi))^{(n+1/2)}} + \frac{(1-\gamma^2)^n}{2\pi}\,F(n;1;1/2\,;\gamma^2\cos^2(\varphi)), \tag{2}$$

where Γ is the Gamma function and F the Gauss hypergeometric function, φ is the phase difference. The phase error standard deviation $\sigma_{\Delta\varphi}$ is depicted in Figure 7.1 for a range of coherences and different number of looks.

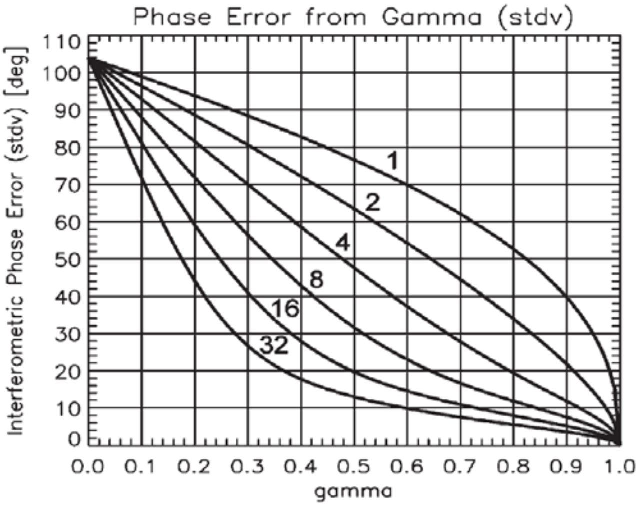

Figure 7.1 Standard deviation of the interferometric phase errors $\sigma_{\Delta\varphi}$, as a function of the total coherence (gamma) and the equivalent number of looks, indicated above each curve [4].

The interferometric phase error directly relates to the relative height accuracy by

$$\Delta h = h_{\mathrm{amb}} \cdot (\,\Delta\varphi/2\pi), \tag{3}$$

where h_{amb} is the height of ambiguity, and represents the height difference corresponding to a complete 2π cycle of the interferometric phase. Naturally, it is crucial – for all interferometric applications – to eliminate phase errors. In consequence of Equation (2) and Figure 7.1, the number of looks and the coherence must be high to minimize interferometric phase errors.

7.1 Number of looks

The number of independent looks is $n = n_{rg} \cdot n_{az}$ giving the product of the number of independent looks in range n_{rg} and the number of independent looks in azimuth n_{az}.

For the generation of the global digital elevation model (DEM) of TanDEM-X, n is typically in the range between 15 and 32.

For a fixed resolution of the interferogram Δrg, Δaz in range and azimuth, respectively, the number of independent looks employed for phase multilooking $n_{rg} = \Delta rg/\delta rg$, $n_{az} = \Delta az/\delta az$ are proportional to the bandwidth in range and azimuth, respectively. δrg and δaz are the SAR image resolution in range and azimuth, respectively. In the following, it will be assumed that the interferometric resolution for azimuth and range are processed to the same spacing, i.e. $\Delta rg = \Delta az = \Delta s$.

The influence of the range spectral filtering on the number of looks will be taken into account in Section 8.

7.2 Interfomeretric coherence

The interferometric coherence can be expressed as the product of different error contribution as follows:

$$\gamma = \gamma_{SNR} \cdot \gamma_{quant} \cdot \gamma_{amb} \cdot \gamma_{rg} \cdot \gamma_{az} \cdot \gamma_{vol} \cdot \gamma_{temp}, \quad (4)$$

where the right-hand side describes the coherence loss due to: limited signal-to-noise ratio (γ_{SNR}), quantization (γ_{quant}), ambiguities (γ_{amb}), baseline decorrelation in range direction (γ_{rg}), relative shift of the Doppler spectra in azimuth direction (γ_{az}), volume decorrelation (γ_{vol}), and temporal decorrelation (γ_{temp}) [4] .

The coherence contributions affected by the transmitted bandwidth are the ones related to the baseline decorrelation, to the SNR, and to the azimuth ambiguities.

8 Impact of range bandwidth on SNR and interferometric phase errors

The commanded chirp pulse bandwidth B_{rg} defines the resolution in range and is directly proportional to the noise equivalent sigma zero (NESZ), which describes the influence of thermal noise contributions in the SAR image [4]. The actual signal-to-noise ratio (SNR) is derived from

$$\mathrm{SNR} = \frac{\sigma_0}{\mathrm{NESZ}}, \tag{5}$$

where σ_0 is the normalized backscattering coefficient. Hence, the SNR decreases with increasing bandwidth. The finite sensitivity of the interferometric SAR system causes a coherence loss [4]

$$\gamma_{SNR} = \frac{1}{\sqrt{(1+\mathrm{SNR}_1^{-1})\cdot(1+\mathrm{SNR}_2^{-1})}}, \tag{6}$$

being $\mathrm{SNR}_{1,2}$ the SNR for each interferometric channel (for both TanDEM-X channels the observed difference in terms of SNR is typically less than 1 dB [6]). Larger receive bandwidths result in larger coherence loss (i.e. smaller values of γ_{SNR}), and vice versa

$$\gamma_{\mathrm{SNR}} \sim \frac{1}{1+\beta B_{rg}}, \tag{7}$$

where β includes all quantities contributing to the SNR except of B_{rg} [4].

On the other hand, the chirp bandwidth B_{rg} employed for a SAR acquisition determines the ground range resolution δrg within each channel, which is expressed by (after spectral filtering [3])

$$\delta rg = \frac{c_0\cdot\cos(\alpha)}{2\cdot B_{rg}\cdot\sin(\theta-\alpha)}\cdot\left|\frac{B_{rg}}{B_{rg}-\Delta f}\right|, \tag{8}$$

where Δf is the spectral shift. The resulting bandwidth available for interferometric processing B_{if} is hence

$$B_{if} = B_{rg}\cdot|1-\Delta f|. \tag{9}$$

The spectral range shift Δf is the difference between the commanded chirp and the interferometric bandwidth. For nominal TanDEM-X digital elevation model stripmap acquisitions 100 MHz chirp bandwidth is commanded, and an interferometric resolution of Δs =12 m for azimuth and range is used for DEM generation. Increasing the range bandwidth implies a proportional improvement in terms of range resolution (and vice versa). For a fixed interferometric resolution Δs, the number of independent range looks employed for phase multilooking n_{rg} is proportional to the interferometric range bandwidth.

$$n_{rg} = \Delta s/\delta rg \sim B_{if} \tag{10}$$

The combined effects of the range bandwidth on the range resolution and on the SNR can be evaluated in Figure 8.1 and Figure 8.2, where the interferometric phase error due to limited SNR is evaluated for different interferometric resolutions Δs = 12 m and Δs = 20 m, respectively, backscatter values σ_0, and spectral range shifts Δf [3], which are likely to occur during the "large baseline" mission phase (baselines of up to 4 km). A clear performance improvement is observed comparing Figure 8.1 with Figure 8.2 when increasing the resulting interferometric resolution Δs, which implies a quadratic increase in terms of number of independent looks, as shown in section 4.1 (please note the different scales of the two plots). For the analysis, an azimuth resolution $\delta az = 6.6$ m has been considered, which corresponds to the theoretical resolution for TanDEM-X dual and quad-pol stripmap acquisitions. For high backscatter values (blue and red rhombi) larger bandwidths are preferred, i.e. the performance is effectively driven by the number of looks. In the case of smaller σ_0 (red and blue circles) the best compromise lies between around 100 and 150 MHz, whereas for larger range bandwidths the limited SNR mainly affects the final performance.

Based on the present results, during the upcoming "large baseline" phase, bistatic acquisitions will be commanded with 150 MHz bandwidth and, if not possible (due to resource limits or other commanding constraints), 100 MHz will be selected. This conclusion is valid for all polarization modes.

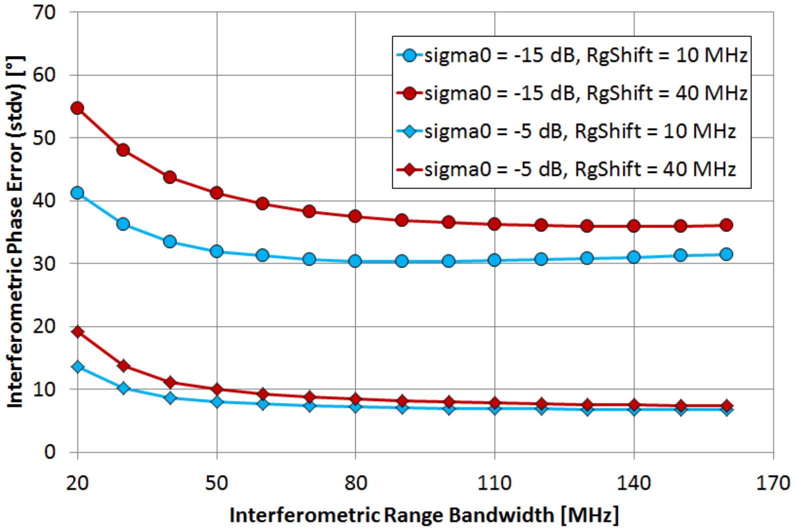

Figure 8.1. Interferometric phase error due to limited SNR $\sigma_{\Delta\varphi,\mathrm{SNR}}$ as a function of interferometric range bandwidth B_{if} (i.e. "net" of the spectral range filtering [3]) for different backscatter values σ_0 and spectral range shifts. For this simulation, the interferometric resolution Δs = 12 m.

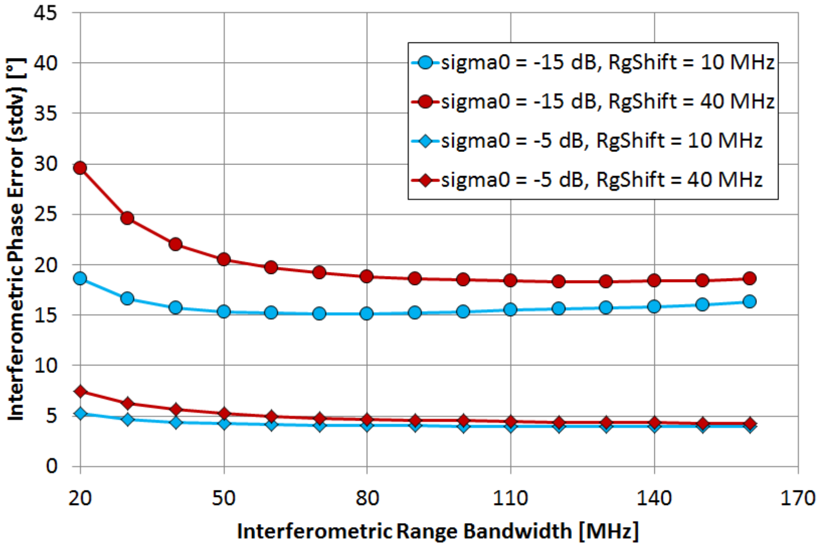

Figure 8.2. Interferometric phase error due to limited SNR $\sigma_{\Delta\varphi,\mathrm{SNR}}$ as a function of interferometric range bandwidth B_{if} (i.e. "net" of the spectral range filtering [3]) for different backscatter values σ_0 and spectral range shifts. For this simulation, the interferometric resolution Δs = 20 m.

9 Impact of processing bandwidth on azimuth ambiguities and interferometric phase errors in quad polarization acquisitions

In TanDEM-X, the processing azimuth bandwidth (PBW) is flexibly adapted to the pulse repetition frequency (PRF) and optimized for the suppression of azimuth ambiguities [6]. The left plot of Figure 9.1 shows the implemented processing bandwidth over PRF. All image pairs processed by the TanDEM-X chain are filtered with this adapted processing bandwidth. For other acquisition modes and certain applications it may be convenient to reprocess the data by the end user with a lower bandwidth. This is specially the case for quad polarization acquisition suffering from stronger ambiguities compared to dual or single polarization acquisitions. Figure 9.1 on the right shows the simulated ratio of the first azimuth ambiguity to the signal ratio (FAASR) considering quad-polarization commanding according and the PBW as shown in the left plot of Figure 9.1. The first azimuth to signal ratio is the main contribution to the azimuth ambiguities. The red line shows the expected FAASR with the nominally implemented processing bandwidth in red.

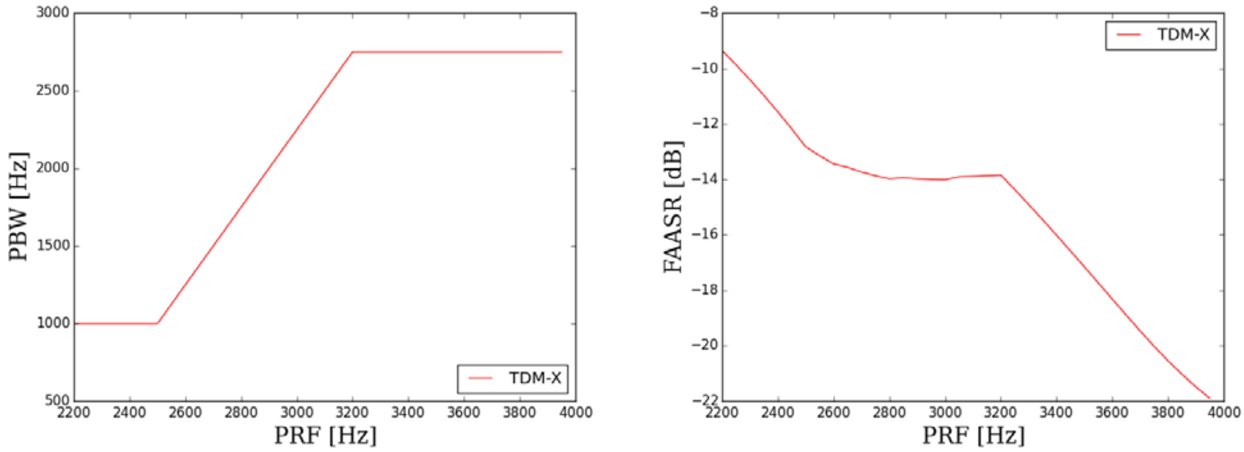

Figure 9.1. Main azimuth ambiguities contribution (first azimuth ambiguity-to-signal ratio, FAASR) for quad pol acquisitions (on the right) and processed azimuth bandwidth (PBW) adapted for the TanDEM-X mission.

The impact of the ambiguities in the coherence product is expressed as:

$$\gamma_{\mathrm{amb}} = \frac{1}{1+RASR} \cdot \frac{1}{1+AASR}, \tag{11}$$

where AASR is the azimuth ambiguity-to-signal ratio and RASR is the range ambiguity-to-signal ratio. To improve the image quality and the coherence, the ambiguities should be supressed as much as possible. In order to reduce the azimuth ambiguities a lower PBW can be used. The decrease of the PBW implies a decrease of the azimuth resolution. Hence, the PBW is directly determining the number of looks in azimuth for fixed spacing.

We considered as AASR only the first ambiguities (FAASR) as main contribution with two backscatter models, two elevations in range and two different resolutions. The next figures show the standard deviation of the interferometric phase error produced by the AASR $\sigma_{\Delta\varphi,\ \mathrm{AASR}}$ for these models for different processing bandwidths derived from Equation (11) and using Equation (2).
Figure 9.2 and Figure 9.3 show on the left the best case, where a homogeneous backscatter is considered and the number of looks in flat angle (30°) acquisitions with of about $n_{rg} = 6$. On the right of Figure 9.2 and Figure 9.3, the worst case is depicted, where the backscatter of the ambiguity is 8 dB higher than in the signal and the number of looks in steep angle (48°) acquisitions with a $n_{rg} = 4$. Figure 9.2 describes the model with interferometric resolution Δs =12 m and the Figure 9.3 with interferometric resolution of Δs =20 m.

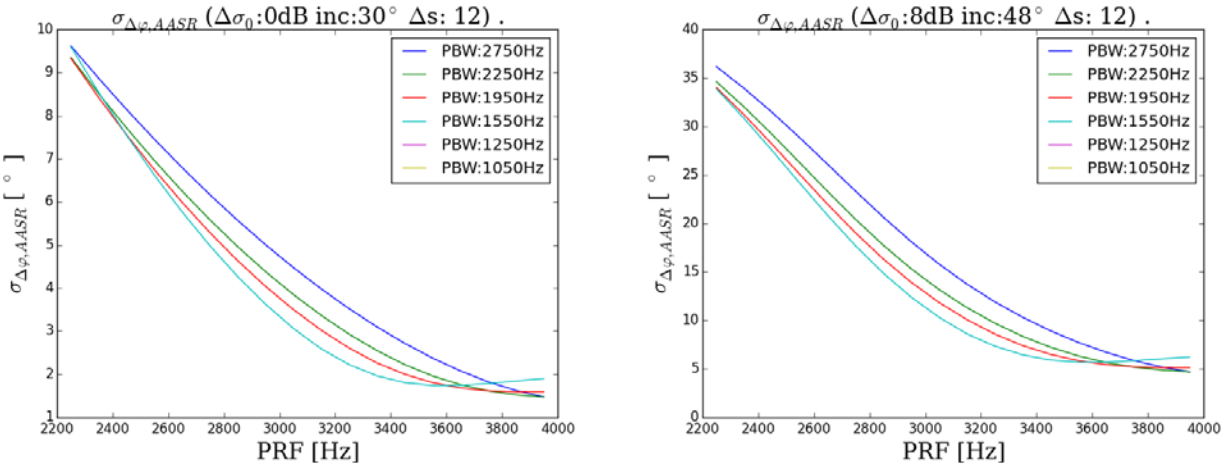

Figure 9.2. Phase error standard deviation due to ambiguities in quad polarization acquisitions and interferometric resolution of 12 m. Two scenarios are depicted: on the left the best case with homogeneous terrain and incidence angle of 30°, and on the right a worsecase with 8 dB higher ambiguities and incidence angle of 48°. Please note the different scales of the two plots.

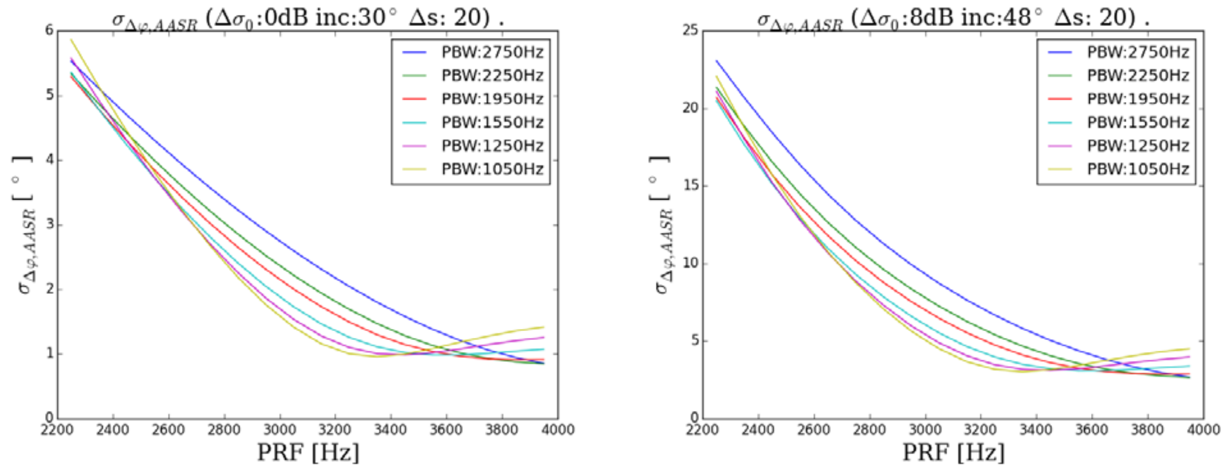

Figure 9.3. Phase error standard deviation due to ambiguities in quad polarization acquisitions and interferometric resolution of 20 m. Two scenarios are depicted: on the left the best case with homogeneous terrain and incidence angle of 30°, and on the right a worse case with 8 dB higher ambiguities and incidence angle of 48°. Please note the different scales of the two plots.

Figure 9.2 and Figure 9.3 show that, for PRFs between about 2400 Hz to 3600 Hz and 2600 Hz to 3400 Hz, respectively, the phase error decreases with increasing PRF and with decreasing processed bandwidth.

The trade-off between a smaller processing bandwidth in order to improve the phase error is optimized for different interferometric resolutions as shown in Figure 9.4. On the left, two quad polarization profiles for processing azimuth bandwidth (PBW) are suggested. The red curve corresponds to the PBW implemented in TanDEM-X, which results from optimizations for single polarisation DEM products. The curves in blue and green corresponds to processing bandwidth for as low as possible phase error product of AASR for interferometric resolution $\Delta s = 12$ and $\Delta s = 20$, respectively. On the right of Figure 9.4, the resulting FAASR for this optimization is depicted.

Figure 9.5 shows phase error product of azimuth ambiguities with the optimized processed bandwidths, for all the above described models. In hand of these results the user can evaluate the need of reprocessing the complex-valued SAR images with another processing bandwidth.

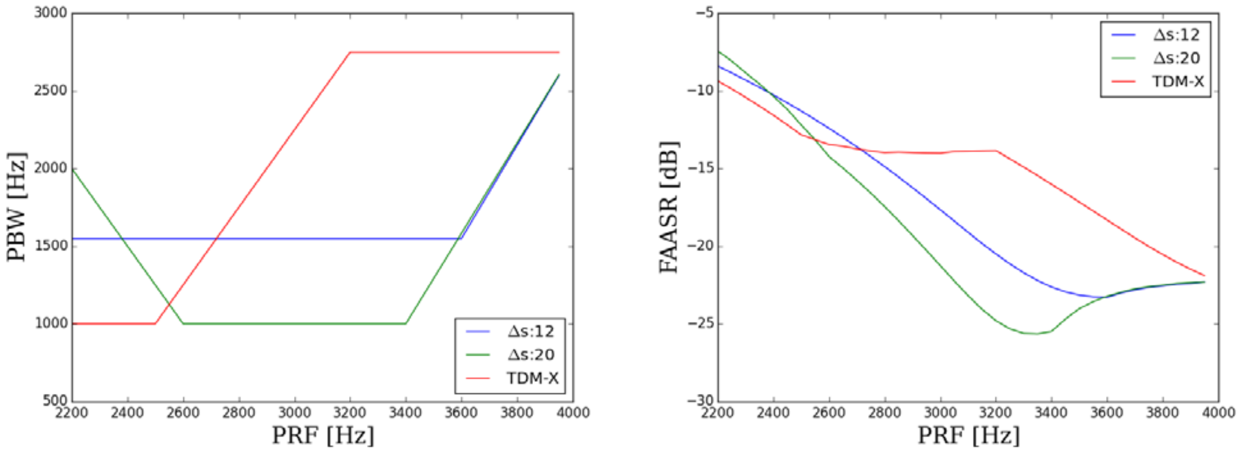

Figure 9.4. (Left) Processed azimuth bandwidth (PBW) adapted to PRF for nominal TanDEM-X mission (red) and recommended for interferometric resolution Δs=12 m (blue) and Δs=20 m (green). (Right) Main azimuth ambiguities contribution (first azimuth ambiguity-to-signal ratio, FAASR) for quad polarization acquisitions.

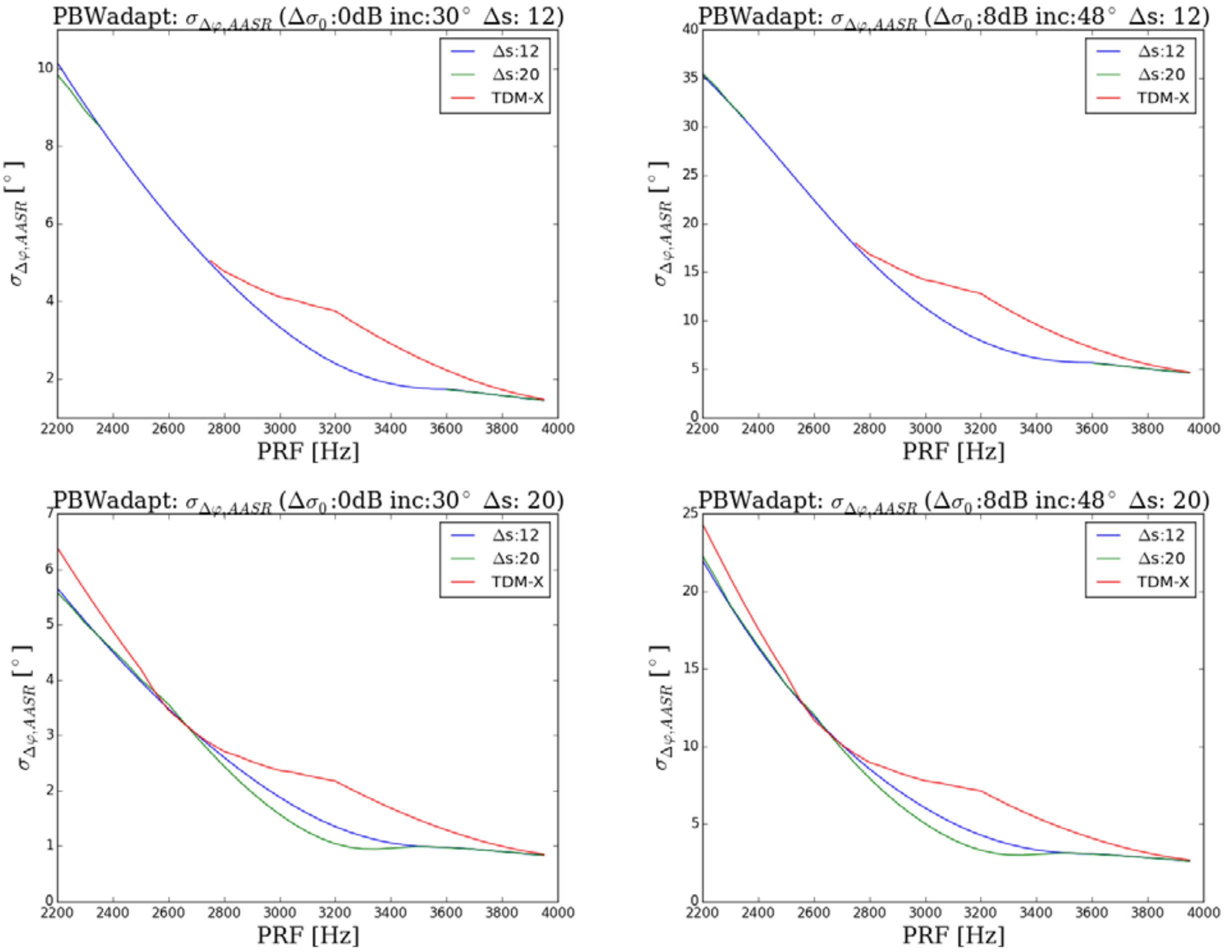

Figure 9.5. Phase error standard deviation due to ambiguities in quad polarization acquisitions and interferometric resolution of 12 m (upper plots) and 20 m (bottom plots). On the left: the best case with homogeneous terrain and incidence angle of 30°, on the right: a worse case with difference of 8 dB and incidence angle of 48°.

10 Conclusions

The TanDEM-X Science Phase is divided into two main sub-phases: Pursuit Monostatic and Bistatic. During the Bistatic sub-phase the baseline between satellites can reach up to 4 km at equator. These large baselines derive in range spectral shift between both channels. As explained in Section 5, filtering the common range bandwith can provoke a significant range resolution loss. Some applications oriented to point targets analysis, such as urban tomography or PSI, would rather prefer to keep the full information. Thus, the CoSSC provided during the Bistatic sub-phase are not filtered in range. In this case, the user is free to perform a range filtering by its own. The coarse DEM provided in the XML "georef.xml" may be used to carry out the range filtering as it is briefly explained in Section 6.2.

The DRA – ATI acquisitions during the Bistatic sub-phase do not present pattern antenna compensation and they are not filtered in azimuth. The purpose is to preserve full information for MTI and ATI applications. Notice that, as explained in Section 6.3, this only applies to combinations of Fore and Aft channels. The SRA combinations provided also in DRA – ATI acquisitions present antenna pattern compensation and azimuth filtering.

The quality of an interferometric data set is mainly characterized by its phase error, which in turn depends on coherence and number of looks. This technical note shows the impact of bandwidth on coherence and number of looks and, consequently, on the interferometric phase error.

The bandwidth of the commanded chirp pulse drives the range resolution and the signal-to-noise ratio (SNR). Furthermore, the interferometric bandwidth is a fraction of the commanded chirp bandwidth after range filtering, which is performed in order to avoid baseline decorrelation. It has been analytically derived that the interferometric phase error has a non-linear dependence on the range bandwidth. Our observations for the TanDEM-X system from Section 8 are:

- An increasing range bandwidth leads to a higher number of looks in range. Thus, a lower phase error is achieved. On the other hand, this degrades the signal-to-noise ratio of the SAR image.
- In principle, data sets with high backscatter values (i.e. high SNR) are less impacted by phase errors compared to low backscatter data.
- The range shift due to baseline decorrelation implies range filtering of the data. The larger the range shift (i.e. the baseline), the higher is the phase error.

The azimuth bandwidth of the data is processed to a fraction of the used pulse repetition frequency (PRF). This suppresses azimuth ambiguities and consequently improves the coherence of the data compared to the use of the full PRF as processing bandwidth. On the other hand, the azimuth resolution is decreased by lowering the processed azimuth bandwidth, which in turn leads to a smaller number of looks in azimuth. Our observations from Section 9 are:

- Lowest phase errors are achieved for highest PRFs. The PRF is selected in the commanding chain of TanDEM-X according to given system and quality constraints.
- The processing bandwidth must be decreased for low PRFs in order to suppress azimuth ambiguities. Overall, the phase error of the interferometric data will benefit from this, although the number of looks is decreased by the lower azimuth resolution.
- Especially for the quad-polarization case, the ambiguities drastically increase. Two dedicated curves for processing bandwidth in azimuth with quad-polarization data have been derived. By

post-processing TanDEM-X SAR images with such azimuth bandwidths, the phase errors can be reduced by several degrees.

We summarize for both bandwidths in range and azimuth:

A high number of looks leads to a lower interferometric resolution, but to a better phase error. We recommend at least five looks, since a very small number of looks drastically degrades the phase quality. The more looks are employed for multilooking, the lower the phase error.

A. Annex. Spectral Filter XML Definition

Schema **spectral_filter_frequencies.xsd**

location:	
schema location:	**D:\docs\tdm\cossc_format\spectral_filter_frequencies.xsd**
attributeFormDefault:	
elementFormDefault:	

Elements	Complex types	Simple types	Attributes
annotationAzimuthSample	T_azimuthBlock	AT_7	name
annotationAzimuthTime	T_azimuthBlockList	T_rangeFiltering	num
annotationRangeSample	T_azimuthFiltering		
annotationRangeTime	T_blockConfig		
azimuthBlock	T_croppedArea		
azimuthBlockList	T_filteringConfig		
azimuthFiltering	T_rangeBlock		
azimuthOverlap	T_rangeBlockList		
azimuthSize	T_scene		
blockConfig	T_spectralShiftFilter_Block		
croppedArea			
dopplerOtherScene			
dopplerShift			
endAzimuthSample			
endRangeSample			
filteringConfig			
firstAzimuthSample			
firstRangeSample			
inputDopplerCentroid			
lastAzimuthSample			
lastRangeSample			
numberAzimuthBlocks			
numberAzimuthSamples			
numberRangeBlocks			
numberRangeSamples			
outputAzimuthBandwidth			
outputDopplerCentroid			
rangeBlock			
rangeBlockList			
rangeFiltering			
rangeOverlap			
rangeSize			
scene			
spectralShiftFilter_Block			
startAzimuthSample			
startAzimuthTime			

startRangeSample
startRangeTime

element **annotationAzimuthSample**

diagram	annotationAzimuthSample
type	**xs:short**
properties	content simple
used by	complexType **T_azimuthBlock**
source	<xs:element name="annotationAzimuthSample" type="xs:short"/>

element **annotationAzimuthTime**

diagram	annotationAzimuthTime
type	**xs:double**
properties	content simple
used by	complexType **T_azimuthBlock**
source	<xs:element name="annotationAzimuthTime" type="xs:double"/>

element **annotationRangeSample**

diagram	annotationRangeSample
type	**xs:short**
properties	content simple
used by	complexType **T_rangeBlock**
source	<xs:element name="annotationRangeSample" type="xs:short"/>

element **annotationRangeTime**

diagram	annotationRangeTime
type	**xs:double**
properties	content simple
used by	complexType **T_rangeBlock**
source	<xs:element name="annotationRangeTime" type="xs:double"/>

element **azimuthBlock**

diagram	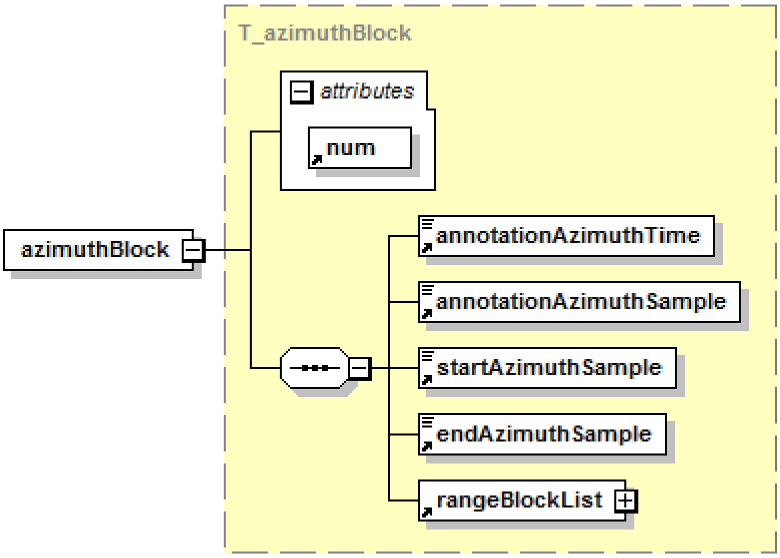
type	T_azimuthBlock
properties	content complex
children	annotationAzimuthTime annotationAzimuthSample startAzimuthSample endAzimuthSample rangeBlockList
used by	complexType T_azimuthBlockList
attributes	Name: num; Type: xs:byte; Use: required; Default: –; Fixed: –; Annotation: –
source	<xs:element name="azimuthBlock" type="T_azimuthBlock"/>

element **azimuthBlockList**

diagram	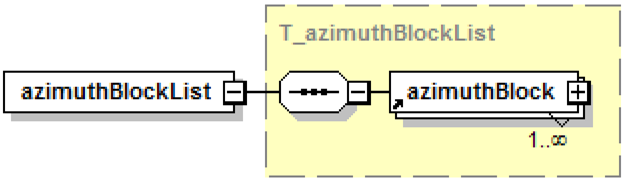
type	T_azimuthBlockList
properties	content complex
children	azimuthBlock
used by	complexType T_scene
source	<xs:element name="azimuthBlockList" type="T_azimuthBlockList"/>

element **azimuthFiltering**

diagram	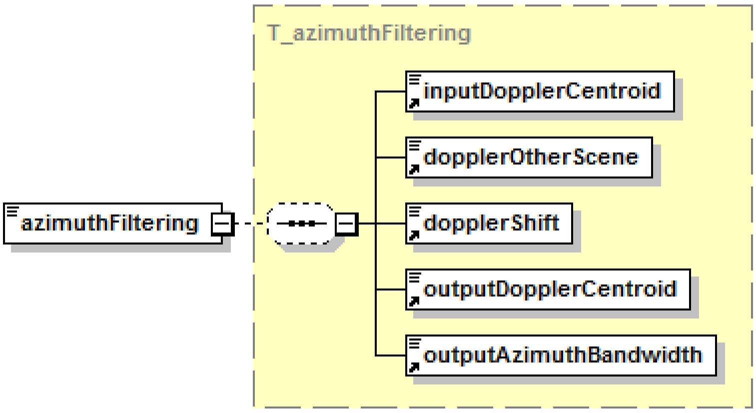
type	**T_azimuthFiltering**
properties	content complex mixed true
children	**inputDopplerCentroid dopplerOtherScene dopplerShift outputDopplerCentroid outputAzimuthBandwidth**
used by	complexTypes **T_filteringConfig T_rangeBlock**
source	<xs:element name="azimuthFiltering" type="T_azimuthFiltering"/>

element **azimuthOverlap**

diagram	
type	**xs:short**
properties	content simple
used by	complexType **T_blockConfig**
source	<xs:element name="azimuthOverlap" type="xs:short"/>

element **azimuthSize**

diagram	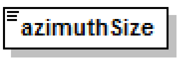
type	**xs:short**
properties	content simple
used by	complexType **T_blockConfig**
source	<xs:element name="azimuthSize" type="xs:short"/>

element **blockConfig**

diagram	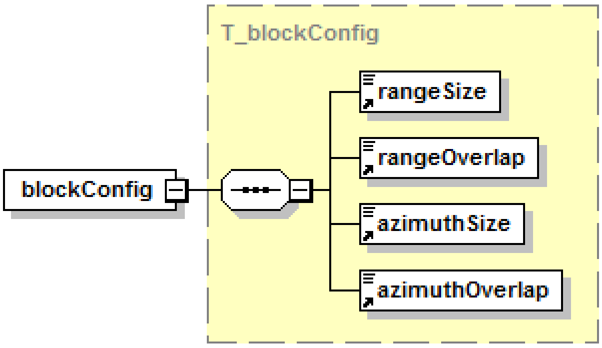
type	**T_blockConfig**
properties	content complex
children	**rangeSize rangeOverlap azimuthSize azimuthOverlap**
used by	complexType **T_spectralShiftFilter_Block**
source	<xs:element name="blockConfig" type="T_blockConfig"/>

element **croppedArea**

diagram	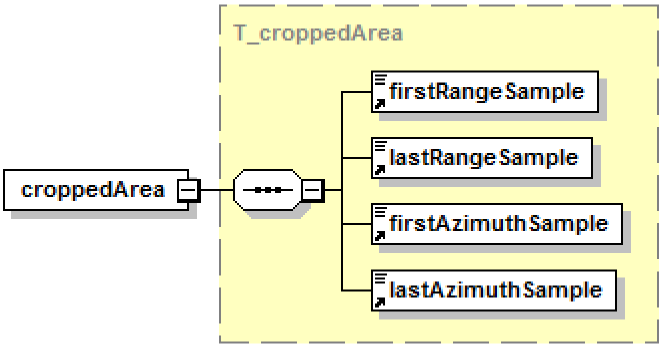
type	**T_croppedArea**
properties	content complex
children	**firstRangeSample lastRangeSample firstAzimuthSample lastAzimuthSample**
used by	complexType **T_scene**
source	<xs:element name="croppedArea" type="T_croppedArea"/>

element **dopplerOtherScene**

diagram	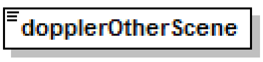
type	**xs:double**
properties	content simple
used by	complexType **T_azimuthFiltering**
source	<xs:element name="dopplerOtherScene" type="xs:double"/>

element **dopplerShift**

diagram	
type	**xs:double**
properties	content simple
used by	complexType **T_azimuthFiltering**
source	<xs:element name="dopplerShift" type="xs:double"/>

element **endAzimuthSample**

diagram	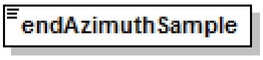
type	**xs:short**
properties	content simple
used by	complexType **T_azimuthBlock**
source	<xs:element name="endAzimuthSample" type="xs:short"/>

element **endRangeSample**

diagram	
type	**xs:short**
properties	content simple
used by	complexType **T_rangeBlock**
source	<xs:element name="endRangeSample" type="xs:short"/>

element **filteringConfig**

diagram	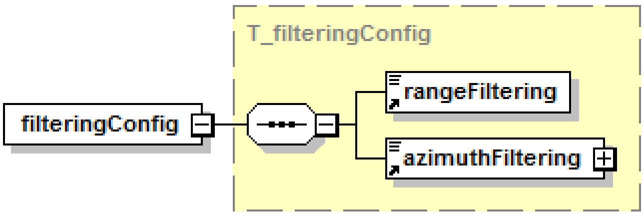
type	**T_filteringConfig**
properties	content complex
children	**rangeFiltering** **azimuthFiltering**
used by	complexType **T_spectralShiftFilter_Block**
source	<xs:element name="filteringConfig" type="T_filteringConfig"/>

element **firstAzimuthSample**

diagram	firstAzimuthSample
type	**xs:byte**
properties	content simple
used by	complexType **T_croppedArea**
source	<xs:element name="firstAzimuthSample" type="xs:byte"/>

element **firstRangeSample**

diagram	firstRangeSample
type	**xs:short**
properties	content simple
used by	complexType **T_croppedArea**
source	<xs:element name="firstRangeSample" type="xs:short"/>

element **inputDopplerCentroid**

diagram	inputDopplerCentroid
type	**xs:double**
properties	content simple
used by	complexType **T_azimuthFiltering**
source	<xs:element name="inputDopplerCentroid" type="xs:double"/>

element **lastAzimuthSample**

diagram	lastAzimuthSample
type	**xs:short**
properties	content simple
used by	complexType **T_croppedArea**
source	<xs:element name="lastAzimuthSample" type="xs:short"/>

element **lastRangeSample**

diagram	lastRangeSample

type	**xs:short**
properties	content simple
used by	complexType **T_croppedArea**
source	<xs:element name="lastRangeSample" type="xs:short"/>

element **numberAzimuthBlocks**

diagram	numberAzimuthBlocks
type	**xs:byte**
properties	content simple
used by	complexType **T_scene**
source	<xs:element name="numberAzimuthBlocks" type="xs:byte"/>

element **numberAzimuthSamples**

diagram	numberAzimuthSamples
type	**xs:short**
properties	content simple
used by	complexType **T_scene**
source	<xs:element name="numberAzimuthSamples" type="xs:short"/>

element **numberRangeBlocks**

diagram	numberRangeBlocks
type	**xs:byte**
properties	content simple
used by	complexType **T_scene**
source	<xs:element name="numberRangeBlocks" type="xs:byte"/>

element **numberRangeSamples**

diagram	numberRangeSamples
type	**xs:short**
properties	content simple
used by	complexType **T_scene**
source	<xs:element name="numberRangeSamples" type="xs:short"/>

element **outputAzimuthBandwidth**

diagram	
type	**xs:double**
properties	content simple
used by	complexType **T_azimuthFiltering**
source	<xs:element name="outputAzimuthBandwidth" type="xs:double"/>

element **outputDopplerCentroid**

diagram	
type	**xs:double**
properties	content simple
used by	complexType **T_azimuthFiltering**
source	<xs:element name="outputDopplerCentroid" type="xs:double"/>

element **rangeBlock**

diagram	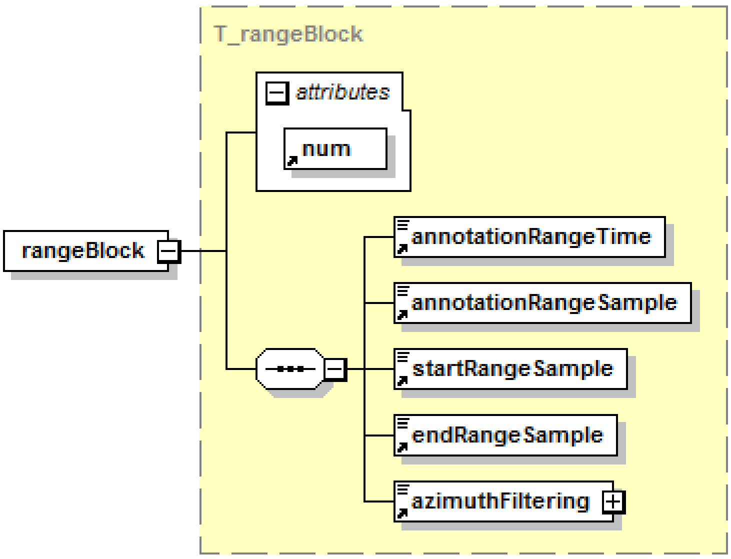
type	**T_rangeBlock**
properties	content complex
children	**annotationRangeTime annotationRangeSample startRangeSample endRangeSample azimuthFiltering**
used by	complexType **T_rangeBlockList**
attributes	Name: num; Type: **xs:byte**; Use: required; Default: ; Fixed: ; Annotation:
source	<xs:element name="rangeBlock" type="T_rangeBlock"/>

element **rangeBlockList**

diagram	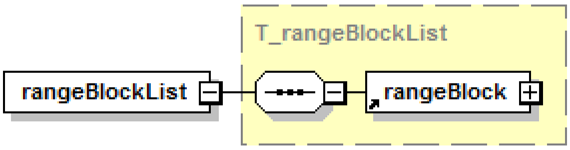
type	**T_rangeBlockList**
properties	content complex
children	**rangeBlock**
used by	complexType **T_azimuthBlock**
source	<xs:element name="rangeBlockList" type="T_rangeBlockList"/>

element **rangeFiltering**

diagram	
type	**T_rangeFiltering**
properties	content simple
used by	complexType **T_filteringConfig**
facets	Kind Value Annotation enumeration Deactivated
source	<xs:element name="rangeFiltering" type="T_rangeFiltering"/>

element **rangeOverlap**

diagram	
type	**xs:byte**
properties	content simple
used by	complexType **T_blockConfig**
source	<xs:element name="rangeOverlap" type="xs:byte"/>

element **rangeSize**

diagram	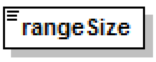
type	**xs:short**
properties	content simple
used by	complexType **T_blockConfig**
source	<xs:element name="rangeSize" type="xs:short"/>

element **scene**

diagram	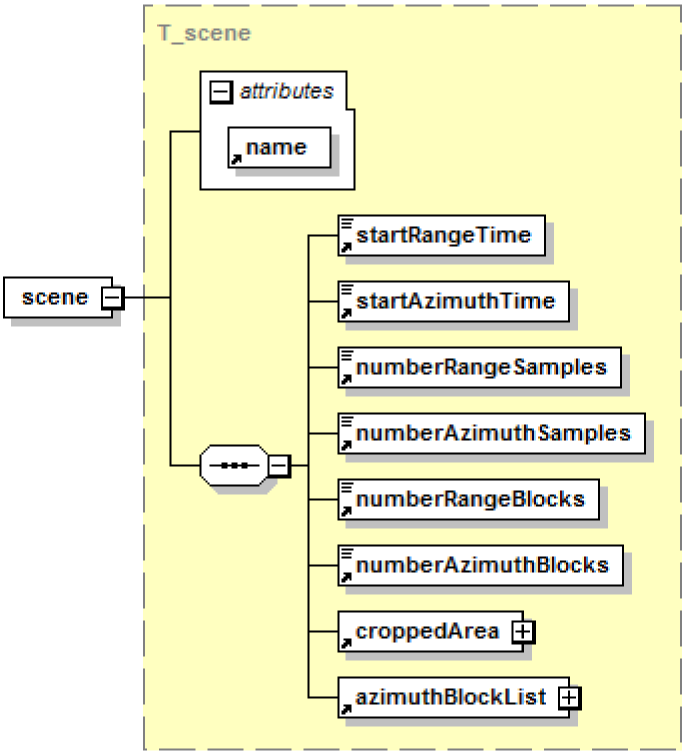
type	T_scene
properties	content complex
children	startRangeTime startAzimuthTime numberRangeSamples numberAzimuthSamples numberRangeBlocks numberAzimuthBlocks croppedArea azimuthBlockList
used by	complexType T_spectralShiftFilter_Block
attributes	Name: name; Type: AT_7; Use: required; Default: ; Fixed: ; Annotation:
source	<xs:element name="scene" type="T_scene"/>

element **spectralShiftFilter_Block**

diagram	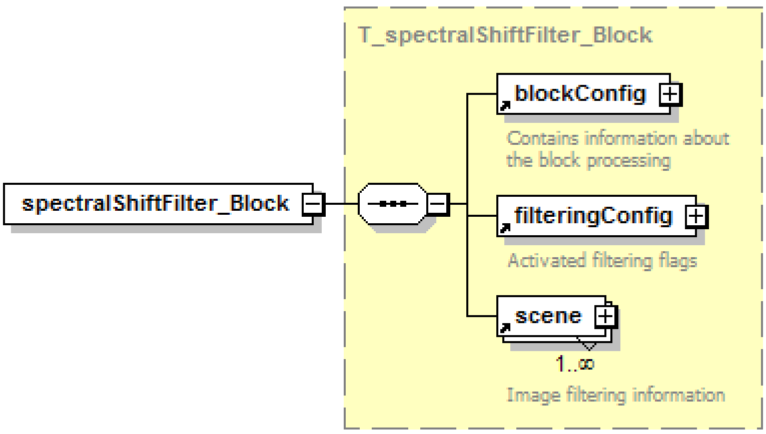
type	T_spectralShiftFilter_Block

properties	content complex
children	**blockConfig** **filteringConfig** **scene**
source	<xs:element name="spectralShiftFilter_Block" type="T_spectralShiftFilter_Block"/>

element **startAzimuthSample**

diagram	startAzimuthSample
type	**xs:short**
properties	content simple
used by	complexType **T_azimuthBlock**
source	<xs:element name="startAzimuthSample" type="xs:short"/>

element **startAzimuthTime**

diagram	startAzimuthTime
type	**xs:double**
properties	content simple
used by	complexType **T_scene**
source	<xs:element name="startAzimuthTime" type="xs:double"/>

element **startRangeSample**

diagram	startRangeSample
type	**xs:short**
properties	content simple
used by	complexType **T_rangeBlock**
source	<xs:element name="startRangeSample" type="xs:short"/>

element **startRangeTime**

diagram	startRangeTime
type	**xs:double**
properties	content simple
used by	complexType **T_scene**
source	<xs:element name="startRangeTime" type="xs:double"/>

complexType **T_azimuthBlock**

diagram

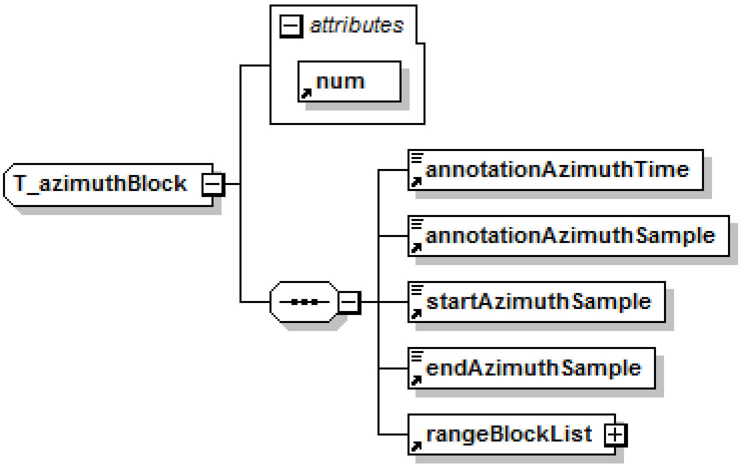

children: **annotationAzimuthTime** **annotationAzimuthSample** **startAzimuthSample** **endAzimuthSample** **rangeBlockList**

used by: element **azimuthBlock**

attributes:

Name	Type	Use	Default	Fixed	Annotation
num	**xs:byte**	required			

source

```
<xs:complexType name="T_azimuthBlock">
  <xs:sequence>
    <xs:element ref="annotationAzimuthTime"/>
    <xs:element ref="annotationAzimuthSample"/>
    <xs:element ref="startAzimuthSample"/>
    <xs:element ref="endAzimuthSample"/>
    <xs:element ref="rangeBlockList"/>
  </xs:sequence>
  <xs:attribute ref="num" use="required"/>
</xs:complexType>
```

complexType **T_azimuthBlockList**

diagram

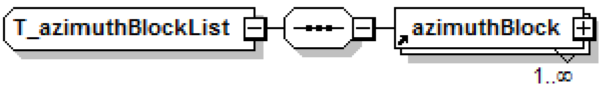

children: **azimuthBlock**

used by: element **azimuthBlockList**

source

```
<xs:complexType name="T_azimuthBlockList">
  <xs:sequence>
    <xs:element ref="azimuthBlock" maxOccurs="unbounded"/>
  </xs:sequence>
</xs:complexType>
```

complexType **T_azimuthFiltering**

diagram	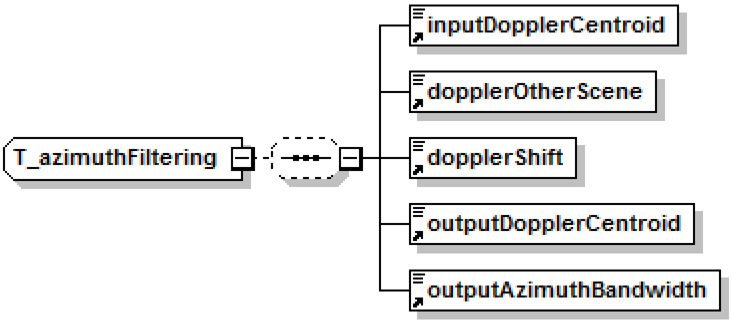
properties	mixed true
children	inputDopplerCentroid dopplerOtherScene dopplerShift outputDopplerCentroid outputAzimuthBandwidth
used by	element azimuthFiltering

source

```
<xs:complexType name="T_azimuthFiltering" mixed="true">
  <xs:sequence minOccurs="0">
    <xs:element ref="inputDopplerCentroid"/>
    <xs:element ref="dopplerOtherScene"/>
    <xs:element ref="dopplerShift"/>
    <xs:element ref="outputDopplerCentroid"/>
    <xs:element ref="outputAzimuthBandwidth"/>
  </xs:sequence>
</xs:complexType>
```

complexType **T_blockConfig**

diagram	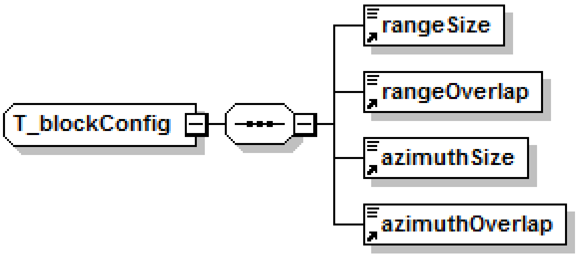
children	rangeSize rangeOverlap azimuthSize azimuthOverlap
used by	element blockConfig

source

```
<xs:complexType name="T_blockConfig">
  <xs:sequence>
    <xs:element ref="rangeSize"/>
    <xs:element ref="rangeOverlap"/>
    <xs:element ref="azimuthSize"/>
    <xs:element ref="azimuthOverlap"/>
  </xs:sequence>
</xs:complexType>
```

complexType **T_croppedArea**

diagram	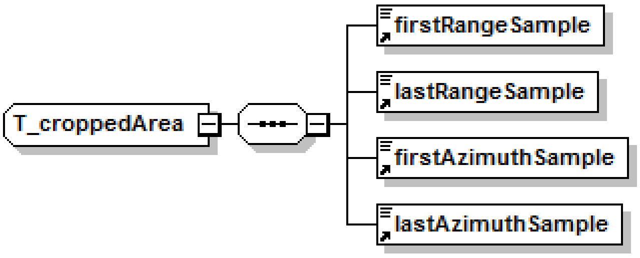
children	firstRangeSample lastRangeSample firstAzimuthSample lastAzimuthSample
used by	element croppedArea

source	`<xs:complexType name="T_croppedArea">`
	`  <xs:sequence>`
	`    <xs:element ref="firstRangeSample"/>`
	`    <xs:element ref="lastRangeSample"/>`
	`    <xs:element ref="firstAzimuthSample"/>`
	`    <xs:element ref="lastAzimuthSample"/>`
	`  </xs:sequence>`
	`</xs:complexType>`

complexType **T_filteringConfig**

diagram	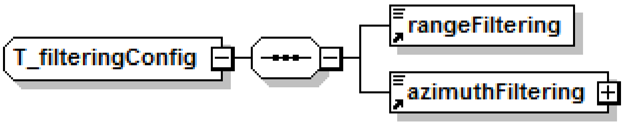
children	rangeFiltering azimuthFiltering
used by	element filteringConfig

source	`<xs:complexType name="T_filteringConfig">`
	`  <xs:sequence>`
	`    <xs:element ref="rangeFiltering"/>`
	`    <xs:element ref="azimuthFiltering"/>`
	`  </xs:sequence>`
	`</xs:complexType>`

complexType **T_rangeBlock**

diagram

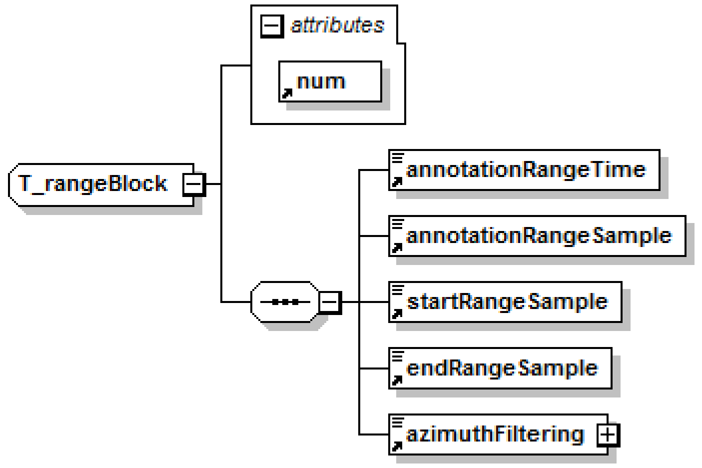

children	annotationRangeTime annotationRangeSample startRangeSample endRangeSample azimuthFiltering					
used by	element **rangeBlock**					
attributes	Name	Type	Use	Default	Fixed	Annotation
	num	**xs:byte**	required			

source

```xml
<xs:complexType name="T_rangeBlock">
  <xs:sequence>
    <xs:element ref="annotationRangeTime"/>
    <xs:element ref="annotationRangeSample"/>
    <xs:element ref="startRangeSample"/>
    <xs:element ref="endRangeSample"/>
    <xs:element ref="azimuthFiltering"/>
  </xs:sequence>
  <xs:attribute ref="num" use="required"/>
</xs:complexType>
```

complexType **T_rangeBlockList**

diagram

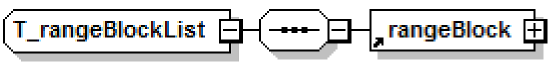

children	rangeBlock
used by	element **rangeBlockList**

source

```xml
<xs:complexType name="T_rangeBlockList">
  <xs:sequence>
    <xs:element ref="rangeBlock"/>
  </xs:sequence>
</xs:complexType>
```

complexType **T_scene**

diagram

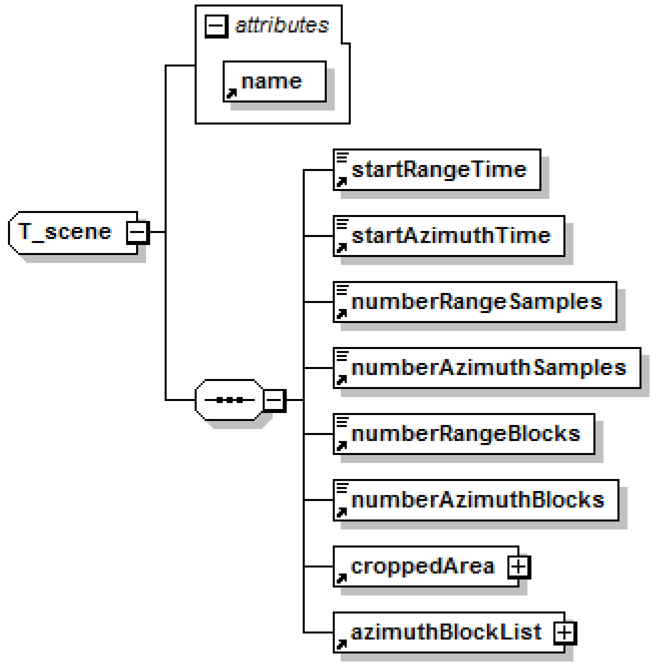

children	startRangeTime startAzimuthTime numberRangeSamples numberAzimuthSamples numberRangeBlocks numberAzimuthBlocks croppedArea azimuthBlockList
used by	element **scene**

attributes

Name	Type	Use	Default	Fixed	Annotation
name	AT_7	required			

source

```
<xs:complexType name="T_scene">
  <xs:sequence>
    <xs:element ref="startRangeTime"/>
    <xs:element ref="startAzimuthTime"/>
    <xs:element ref="numberRangeSamples"/>
    <xs:element ref="numberAzimuthSamples"/>
    <xs:element ref="numberRangeBlocks"/>
    <xs:element ref="numberAzimuthBlocks"/>
    <xs:element ref="croppedArea"/>
    <xs:element ref="azimuthBlockList"/>
  </xs:sequence>
  <xs:attribute ref="name" use="required"/>
</xs:complexType>
```

complexType **T_spectralShiftFilter_Block**

diagram

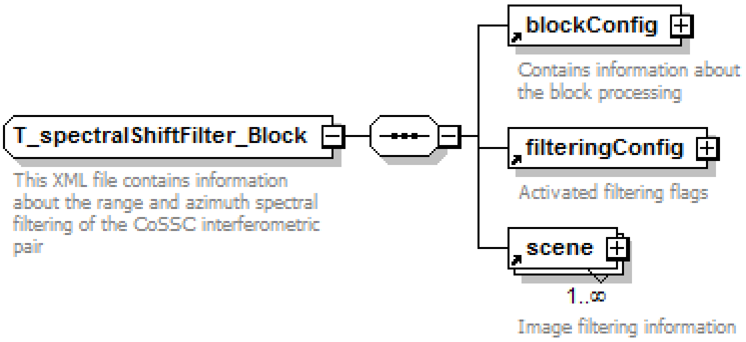

children	**blockConfig** **filteringConfig** **scene**
used by	element **spectralShiftFilter_Block**
annotation	documentation This XML file contains information about the range and azimuth spectral filtering of the CoSSC interferometric pair

source

```
<xs:complexType name="T_spectralShiftFilter_Block">
  <xs:annotation>
    <xs:documentation>This XML file contains information about the range and azimuth spectral filtering of the CoSSC interferometric pair</xs:documentation>
  </xs:annotation>
  <xs:sequence>
    <xs:element ref="blockConfig">
      <xs:annotation>
        <xs:documentation>Contains information about the block processing</xs:documentation>
      </xs:annotation>
    </xs:element>
    <xs:element ref="filteringConfig">
      <xs:annotation>
        <xs:documentation>Activated filtering flags</xs:documentation>
      </xs:annotation>
    </xs:element>
    <xs:element ref="scene" maxOccurs="unbounded">
      <xs:annotation>
        <xs:documentation>Image filtering information</xs:documentation>
      </xs:annotation>
    </xs:element>
  </xs:sequence>
</xs:complexType>
```

simpleType **AT_7**

type	restriction of **xs:string**
properties	base xs:string
used by	attribute **name**

facets

Kind	Value	Annotation
enumeration	FILT.1	
enumeration	FILT.2	

source

```
<xs:simpleType name="AT_7">
  <xs:restriction base="xs:string">
    <xs:enumeration value="FILT.1"/>
    <xs:enumeration value="FILT.2"/>
  </xs:restriction>
```

	</xs:simpleType>

simpleType **T_rangeFiltering**

type	restriction of **xs:string**
properties	base xs:string
used by	element **rangeFiltering**
facets	Kind Value Annotation enumeration Deactivated
source	<xs:simpleType name="T_rangeFiltering"> <xs:restriction base="xs:string"> <xs:enumeration value="Deactivated"/> </xs:restriction> </xs:simpleType>

attribute **name**

type	**AT_7**
used by	complexType **T_scene**
facets	Kind Value Annotation enumeration FILT.1 enumeration FILT.2
source	<xs:attribute name="name" type="AT_7"/>

attribute **num**

type	**xs:byte**
used by	complexTypes **T_azimuthBlock** **T_rangeBlock**
source	<xs:attribute name="num" type="xs:byte"/>